Candidate molecular ions for an electron electric dipole moment experiment

Edmund R. Meyer* and John L. Bohn
Department of Physics, JILA, National Institute of Standards and Technology and University of Colorado, Boulder, Colorado 80309-0440, USA

Michael P. Deskevich
Department of Chemistry and Biochemistry, JILA, National Institute of Standards and Technology and University of Colorado, Boulder, Colorado 80309-0440, USA

(Received 10 March 2006; published 12 June 2006)

This paper is a theoretical work in support of a newly proposed experiment [R. Stutz and E. Cornell, Bull. Am. Soc. Phys. **89**, 76 (2004)] that promises greater sensitivity to measurements of the electron's electric dipole moment (EDM) based on the trapping of molecular ions. Such an experiment requires the choice of a suitable molecule that is both experimentally feasible and possesses an expectation of a reasonable EDM signal. We find that the molecular ions PtH^+ and HfH^+ are both suitable candidates in their low-lying $^3\Delta$ states. In particular, we anticipate that the effective electric fields generated inside these molecules are approximately 73 and −17 GV/cm, respectively. As a byproduct of this discussion, we also explain how to make estimates of the size of the effective electric field acting in a molecule, using commercially available nonrelativistic molecular structure software.

DOI: 10.1103/PhysRevA.73.062108 PACS number(s): 11.30.Er, 31.15.Ar, 31.50.Bc

I. INTRODUCTION

The standard model of elementary particle physics admits that the electron may have an electric dipole moment (EDM), but a very small one; the standard model prediction is on the order of $d_e = 10^{-38}$ e cm, many orders of magnitude below the current experimental limit. Nevertheless, in models beyond the standard model, notably supersymmetry, a larger EDM is expected, sometimes tantalizingly close to the current experimental upper bounds on d_e [1]. To observe d_e would imply a different form of charge-conjugation and/or parity (CP) violation than the familiar form in the K- and B-meson systems. The observation of d_e requires extremely large electric fields to observe the energy shift due to different alignments of d_e along the quantization axis.

The current upper limit on the electron EDM, 1.6×10^{-27} e cm, comes from measurements in atomic thallium [2]. In this experiment, an *effective* electric field is generated inside the atom. The magnitude of this electric field (on the order of 70 MV/cm) is far larger than the field that could be applied directly in the laboratory. This circumstance is what makes an atomic EDM experiment desirable.

Taking this idea even further, Sandars noted that the effective electric field within a molecule can be even larger than that within an atom [3]. This insight has prompted a series of proposed and actual experiments, aimed at using molecules as high-electric-field laboratories. These experiments have employed either molecular beams or traps for neutral molecules, including molecules PbO [4,5] and YbF [6,7]. Several others have also been proposed as viable candidates [8–13].

Recently, a new experiment has been proposed that may increase the experimental sensitivity to an electron EDM by orders of magnitude [14,15]. The key to this experiment is using molecular ions in lieu of neutral molecules. Because ions are far easier to trap for long times than neutrals, the proposed experiment wins in terms of long coherence times. Nevertheless, such an experiment poses a number of challenges, both in experimental technology and in the choice of a reasonable molecule.

The purpose of this paper is to identify diatomic molecular ions that possess properties that are desirable for this experiment. For instance, the molecule should have a relatively small degeneracy of quantum mechanical states near its ground state. This feature, in a cold sample at thermal equilibrium, would ensure that most or all of the ions are already in or near a state that is useful for the EDM measurement. Because the number of ions in a trap is fairly small, this requirement is necessary for achieving a good signal-to-noise ratio. To meet this requirement we restrict our attention to diatomic hydrides, where the light hydrogen atom will contribute to a relatively large rotational constant. Similarly, we are interested in heavy atoms with spinless isotopes in order to ensure a favorable population distribution. This requirement is an experimental one. On the theory side, isotopes with spin are useful in characterizing the accuracy of the calculations and for making empirical estimates [4,13]. A second requirement is that the electric field used to polarize the molecule must be relatively small, on the order of 100 V/cm or less. This is because in the proposed experiment, the polarizing field must be rotating at MHz frequencies in order to act on the molecules without accelerating them out of the trap. Last, we restrict ourselves to molecules that have at least one unpaired spin (paramagnetic, i.e., molecules with $S \neq 0$), so that the net EDM of the electrons does not vanish.

Because we confine our attention to diatomic molecules, we must meet two additional requirements: (1) a large dipole moment, on the order of 1 D, which is not hard to achieve if the two atoms are quite different, and (2) a small energy

*Electronic address: meyere@murphy.colorado.edu

splitting between even- and odd-parity branches of the ground state. In other words, a small omega doublet is desirable.

In general, the size of the omega doublet is smaller for a larger quantum number Ω, which represents the total (orbital plus spin) angular momentum of the electron about the intermolecular axis. For this reason we prefer diatomic molecules with a high angular momentum. In the following we consider species with $^3\Delta$ molecular symmetry, which can support values of Ω as large as $\Omega=3$. This choice is in sharp contrast with previous EDM candidate molecules, most of which were based on $^2\Sigma$ molecular symmetries. More recently, molecules of $^3\Sigma$ [4,5] or $^2\Pi$ [12,13] symmetry have been considered as well.

Finally, the essential requirement for the molecule is that it must possess a large internal effective electric field. It is this field that acts on the electron's EDM to make a measurable signal. A quick review of the relevant physics reveals why a large internal field is so important. If an electric field were applied to an atom, and if relativity did not matter, then a given electron would feel no net electric field. In equilibrium, the applied external field would be exactly balanced by the field due to all the other charges in the atom, or else the electron would be pulled to a different equilibrium. This is the content of Schiff's theorem [16]. However, the fact that the electron can move at relativistic speeds in an atom provides a loophole around this theorem. In the relativistic case, the electron's equilibrium is governed by the balance of electric fields, plus the motional magnetic field generated when it swings by the nucleus. Thus the net electric field, by itself, can be nonvanishing. By applying an external electric field, the nonzero field within the molecule can be increased by a relativistic enhancement factor manifested through the mixing of s and p atomic states. The resulting energy shift scales with the third power of the nuclear charge, and therefore strongly favors heavy atoms as EDM candidates.

Qualitatively, molecules can be even more effective at mixing s and p states of atoms than externally applied fields. Indeed, in molecular orbitals it is possible for s and p levels to perfectly hybridize, as in the conjugated bonds of carbon-bearing molecules. The relativistic enhancement factor can be estimated from its value for the heavy atom, therefore estimating the effective internal electric field becomes a question for the nonrelativistic molecular structure theory. The mixing of s and p atomic orbitals is useful only when it produces a molecular orbital of σ symmetry. An electron in such a molecular orbital has no orbital angular momentum about the molecular axis, and can thus penetrate close to the heavy atom's nucleus, where relativistic effects are greatest. This behavior explains why molecules with total symmetry Σ have been preferred in the past.

As noted above, however, the experiment under consideration is likely constrained to molecules with *nonzero* angular momentum about the axis. To accomplish these seemingly contradictory goals, we seek molecules having two valence electrons. One, of σ molecular symmetry, will be responsible for the effective electric field and consequent EDM signal. The second, of δ symmetry, will allow for small omega doubling. We are thus led to contemplate molecules of $(\sigma\delta)^3\Delta_\Omega$ symmetry overall. Further, since δ molecular orbitals are likely to arise from d-type atomic orbitals, we seek diatomic molecules in which the heavy atom is a transition metal. Previous theoretical work on heavy transition metal hydrides [17] identifies a pair of likely molecules with low-lying $^3\Delta$ states, namely, HfH^+ and PtH^+.

In the following sections we will explore the properties of these and other molecules in terms of their usefulness to an electron EDM experiment. In Sec. II we revisit the theoretical methods for estimating the EDM signal in terms of nonrelativistic molecular wave functions and the way in which such wave functions can be constructed. In Sec. III we present concrete examples of calculations for various diatomic molecules. These calculations verify that the perturbative methods which we employ can semiquantitatively reproduce the effective electric fields predicted previously by more substantial calculations.

II. BACKGROUND: OBSERVABLE CHARACTERISTICS OF THE ELECTRON EDM

A. The effective electric dipole moment of an atom

In EDM circles, it is customary to speak of an "effective electric field" experienced by the electron inside an atom or molecule. What this means in practice is that the energy shift due to an electron EDM of magnitude d_e is simply

$$\Delta E = -d_e F_{\text{eff}}. \tag{1}$$

We use the letter F to denote electric field strengths, to distinguish them from energies, denoted E. To evaluate the energy shift, one writes that the perturbation Hamiltonian in Dirac notation ([18], p. 254 ff.)

$$H_d = \begin{pmatrix} 0 & 0 \\ 0 & 2d_e\boldsymbol{\sigma}\cdot\mathbf{F} \end{pmatrix}. \tag{2}$$

This 2×2 matrix acts on the state vector $\psi=(\psi_U,\psi_L)$, where ψ_U and ψ_L are the "upper" and "lower" components of the electron's Dirac wave function. Each of ψ_U and ψ_L, in turn, stands for a two-component spinor.

In Eq. (2), σ is a Pauli matrix designating the electron's spin, so the combination $d_e\sigma$ describes the EDM of the electron. (The direction of the electron's EDM is presumed to be collinear with its magnetic moment.) This moment interacts with the instantaneous electric field $\mathbf{F}$ experienced by the electron. To a good approximation, this field is given by the Coulomb field of the heavy nucleus with charge Ze, $\mathbf{F}=Ze\hat{r}/r^2$. Here r is the electron-heavy atom distance. Here and throughout this paper we use atomic units, setting $\hbar=m_e=1$.

Next we denote the lower component of the electron's ground state wave function to be $|\psi_L^0\rangle$. Then the perturbative energy shift due to H_d would be $\langle\psi_L^0|2d_e\sigma\cdot\mathbf{F}|\psi_L^0\rangle$. However, this expression vanishes for a ground-state wave function of definite parity, owing to the odd-parity of $\mathbf{F}$. Thus, an externally applied electric field is required to mix states of different parities. In the important example of an atom with an s electron (e.g., Cs), an applied electric field would create a linear combination of s and p states,

$$|\psi_L^0\rangle = \epsilon_s|\psi_L(s)\rangle + \epsilon_p|\psi_L(p)\rangle. \quad (3)$$

Higher angular momentum states are also possible, in principle, but do not make a substantial contribution at laboratory fields. In typical atomic EDM experiments, the field is sufficiently weak to invoke the perturbative approximations:

$$\epsilon_s \approx 1, \quad (4)$$

$$\epsilon_p \approx \frac{\langle s|e\mathbf{r}\cdot\mathbf{F}_{\text{applied}}|p\rangle}{E(s)-E(p)}. \quad (5)$$

Here $e\mathbf{r}$ stands for the relevant dipole operator, and the denominator denotes the energy difference between the s and p states.

With these approximations, the expression for the energy shift becomes

$$\langle\psi_L^0|2d_e\sigma\cdot\mathbf{F}|\psi_L^0\rangle = 2\epsilon_s\epsilon_p\left(\frac{d_eZe}{a_0^2}\right)\Gamma_{\text{rel}}. \quad (6)$$

The factor Γ_{rel} incorporates the relativistic effects and can be estimated analytically using the relativistic Coulomb wave functions [18]:

$$\Gamma_{\text{rel}} = a_0^2\left\langle s_{1/2}\left|\frac{2\sigma\hat{r}}{r^2}\right|p_{1/2}\right\rangle = -\frac{4(Z\alpha)^2Z_i^2}{\gamma(4\gamma^2-1)(\nu_s\nu_p)^{3/2}}, \quad (7)$$

where α is the fine structure constant and $\gamma = \sqrt{(j+1/2)^2-(Z\alpha)^2}$. The quantities ν_s and ν_p are the effective quantum numbers for the s and p states of the heavy atom, defined as the the principal quantum number shifted by a quantum defect. All values of ν_s and ν_p are obtained from Ref. [19]. The constant Z_i is the effective nuclear charge seen by the valence electron; for a neutral atom $Z_i=1$. An additional energy shift would arise from perturbations due to the $p_{3/2}$ excited state. However, the matrix element connecting the $s_{1/2}$ state to the $p_{3/2}$ state is vanishingly small, since the $p_{3/2}$ radial function has negligible amplitude near the nucleus [20].

The energy shift of an atom in an electric field, due to the EDM of the electron, thus requires mixing the $s_{1/2}$ ground state and the $p_{1/2}$ excited state. The resulting energy shift is, in atomic units,

$$\Delta E = \left[\frac{4\langle s_{1/2}|z|p_{1/2}\rangle}{E(s_{1/2})-E(p_{1/2})}\Gamma_{\text{rel}}\frac{Ze^2}{a_0^2}\right]d_eF_{\text{applied}}. \quad (8)$$

This expression can be viewed in two ways. One way is to envision that the atom gains an EDM that is bigger than the electron's EDM by the factor in square brackets in Eq. (8). Alternatively, the existing electronic EDM may be seen as experiencing the applied field F_{applied}, enhanced by this same factor.

B. The effective electric field inside a molecule

In diatomic molecules, the same kind of s-p mixing may occur, perhaps much more substantially than in an atom [21,22]. If so, the basic expression for the measured energy shift is still given by Eq. (6), but the coefficients may have quite different values. To estimate these coefficients, we expand the molecular orbital wave function of the contributing electron in terms of atomic orbitals:

$$|\text{mol}\rangle = \epsilon_s|s\rangle + \epsilon_p|p\rangle + \sum_{\text{other}}\epsilon_{\text{other}}|\text{other}\rangle. \quad (9)$$

Here s and p still refer to the relevant atomic orbitals on the heavy atom, from which the EDM shift will arise. But now there are other orbitals that may participate. For example, the electron wave function may have considerable contributions from d or f orbitals on the heavy atom or from atomic orbitals residing on the other atom. Thus, in general, it may *not* be a good approximation that $\epsilon_s^2+\epsilon_p^2=1$. Nevertheless, one may seek molecules for which $|\epsilon_s| \approx |\epsilon_p| \approx 1/\sqrt{2}$, which would be the optimal mixing for our purposes. To determine these quantities for a given molecule is a problem in nonrelativistic molecular orbital theory.

Once the amplitudes ϵ_s and ϵ_p are known, we can use Eq. (6) to find the energy shift, with the following caveat. The orbital $|p\rangle$ here stands for the nonrelativistic p wave function of the atom. It is therefore a linear combination of the relativistic atomic states, denoted by total spin j:

$$|p\rangle = -\frac{2\sigma}{\sqrt{3}}|p_{1/2}\rangle + \sqrt{\frac{2}{3}}|p_{3/2}\rangle. \quad (10)$$

The factor 2σ emphasizes that the $p_{1/2}$ contributes with opposite signs for the two spin projections on the molecular axis, $\sigma=\pm1/2$. As noted above, the $p_{3/2}$ orbital does not contribute to the electron EDM shift; hence the relevant matrix element reads

$$\langle s|2d_e\sigma\cdot\mathbf{F}|p\rangle = -\frac{2\sigma}{\sqrt{3}}\langle s_{1/2}|2d_e\sigma\cdot\mathbf{F}|p_{1/2}\rangle. \quad (11)$$

Thus, following Flambaum [21] and Khriplovich and Lamoreaux [22], we find the electron EDM energy shift for a diatomic molecule (in atomic units):

$$\Delta E = -\left[\frac{4\sigma}{\sqrt{3}}\epsilon_s\epsilon_p\Gamma_{\text{rel}}\frac{Ze^2}{a_0}\right]\frac{d_e}{ea_0}. \quad (12)$$

In a strong contrast to Eq. (8), the molecular expression Eq. (12) does *not* depend explicitly on the applied electric field $\mathbf{F}_{\text{applied}}$. The effective electric field is simply the coefficient in front of d_e. Applying an external field in the laboratory is essential, however. In zero electric field, the molecule's energy eigenstates are also eigenstates of parity [23]:

$$||\Omega|,\pm\rangle = \frac{1}{\sqrt{2}}(|\Omega\rangle \pm |-\Omega\rangle), \quad (13)$$

but separated by an energy E_{doub} referred to as the Ω-doubling energy. By convention, the lower (upper) sign of this doublet is denoted by the letter e (f). In such a state, the electronic spin projection σ will lie along the molecular dipole moment as often as against it, canceling the energy shift. However, in a modest electric field $\mathbf{F}_{\text{applied}}$, the signed values of $\pm\Omega$ are again good quantum numbers, and the expression Eq. (12) is relevant. To overcome E_{doub}, the field must be large compared to a "critical" field, at which the

Stark energy overcomes the energy difference between the two parity eigenstates:

$$F_{\mathrm{crit}} = \frac{E_{\mathrm{doub}}}{d_M}, \tag{14}$$

where d_M is the permanent electric dipole moment of the molecule. For the proposed molecular ion experiment, it is desirable to make F_{crit} as small as possible, preferably below 100 V/cm [14].

III. COMPUTATIONAL METHOD

There remains the question of evaluating the constants ϵ_s and ϵ_p for a given molecule of interest. Fortunately, it is common practice in the molecular structure theory to cast molecular orbitals as linear combinations of atomic orbitals. The atomic orbitals, in turn, are usefully expressed in terms of a Gaussian basis set that is carefully constructed to reproduce the energy levels of the individual atoms. After decades of development, these methods are now robust and commercially available in software packages such as GAUSSIAN [24] and MOLPRO [25]. We use MOLPRO in the calculations performed here.

A. Molecular electronic structure

We assume that the molecules are well-approximated by Hund's angular momentum coupling case (a). This approximation is justified by the much greater strength of the spin-orbit interaction and the exchange splitting (both on the order of 10^3 cm^{-1}) as compared to rotational energies (on the order of 10 cm^{-1}). In this case the relevant quantum numbers of each electron are its projection of orbital (λ) and spin (σ) angular momentum on the molecular axis. [In fact, strong spin-orbit mixing will impact these quantum numbers slightly, pushing the molecules toward Hund's case (c). We will deal with this later.]

To make a concrete calculation, each molecular orbital is expanded in a basis set of Gaussian functions, where a basis element is defined as

$$|b_j\rangle = \sum_i s_i |g_i\rangle. \tag{15}$$

Here each $|g_i\rangle$ is a Gaussian function centered on either of the atoms in the molecule. Such a set of Gaussians is chosen to optimize the energies of each atom separately and is provided in one of a set of standard basis sets, referred to below. With this basis, it is now possible to define an orbital as

$$|\phi_k\rangle = \sum_j c_j |b_j\rangle, \tag{16}$$

and a configuration is a product of occupations of orbitals given as

$$|\Phi_l\rangle = \mathcal{A} \prod_k d_k |\phi_k\rangle. \tag{17}$$

The d_k can take the values 0,1, or 2. $\mathcal{A}$ stands for antisymmetrization.

The Hartree-Fock procedure minimizes the energy of the ground-state configuration, hence only one configuration is optimized. This is done by minimizing the coefficients in the orbitals and configurations. For concreteness, the configuration is

$$|\Phi^{\mathrm{HF}}\rangle = \prod_k d_k \sum_j c_{kj} |b_j\rangle, \tag{18}$$

and the procedure finds the d_k and c_{kj} that minimize the total electronic energy E. After this procedure, we perform a multiconfiguration self-consistent field (MCSCF) [26,27] calculation with a complete active space within MOLPRO. The MCSCF takes the HF E as an initial guess and finds appropriate linear combinations of the configurations given in Eq. (18) that minimize E over M configurations. The M configurations can contain many different symmetries and spin states. This wave function is

$$|\Phi^{\mathrm{MCSCF}}\rangle = \sum_l f_l |\Phi_l\rangle = \sum_l f_l \prod_k d_{lk} \sum_j c_{kj} |b_j\rangle, \tag{19}$$

and the procedure varies f_l, d_{lk}, and c_{kj} in order to minimize the average E. This is the time-consuming part of the calculation due to the nonlinear optimization routine. This step is then followed by the multireference configuration interaction (MRCI) [28,29] program. A MRCI calculation uses the MCSCF configurations and mixes in single and double excitations. The wave function is

$$|\Psi^{\mathrm{MRCI}}\rangle = \sum_m h_m |\Phi_m^{\mathrm{MCSCF}}\rangle, \tag{20}$$

where this procedure finds the h_m that minimize the value of E for a given symmetry, subject to the constraint that the f_l, d_{lk}, and c_{kj} are all fixed.

Therefore, deep inside the MCSCF wave function is the σ molecular orbital that mixes the atomic s and p orbitals. We denote this orbital as $|\mathrm{mol}, \sigma\rangle$, which has an explicit expansion into the Gaussian basis functions according to Eq. (18). Analogously, the wave function for the heavy atom (e.g., Hf^+ or Pt^+) is also computed at the MCSCF and MRCI levels and contains atomic orbitals $|\mathrm{atom}, s\rangle$ and $|\mathrm{atom}, p\rangle$ expanded into the *same* Gaussian basis set. It is now straightforward to estimate the amplitudes $\epsilon_{s,p} = \langle \mathrm{mol} | \mathrm{atom}, (s,p) \rangle$.

There are two final, but sometimes decisive, corrections. First, the desired configuration does not constitute the entire wave function, but only a fraction of it, given by its amplitude, e.g., h_0 in the MRCI expansion in Eq. (20). For the molecules considered in the proposed experiment, however, we have found this factor to be within several percent of unity. Alternatively, it does play a crucial role in the case of PbO where the factor h_0 is considerably less than unity for the $(\sigma\sigma^*)^3\Sigma$ metastable state; the state that contributes to the EDM signal.

More significantly, the molecular state identified in Eq. (20) may be mixed with others via spin-orbit couplings. In the case that one other molecular symmetry is mixed in, we get

$$|\Psi\rangle = \cos\chi \,|^{2S+1}\Lambda\Sigma, \Omega\rangle + \sin\chi \,|^{2S'+1}\Lambda'\Sigma', \Omega\rangle, \tag{21}$$

in terms of a mixing angle χ. There is no prime on the Ω since spin-orbit interactions preserve the value of Ω. The factor $\cos\chi$ can be quite significant. For example, in a $^2\Pi$ state (as in PbF [10] and the Halides HBr^+ [12] and HI^+ [12,13]), the single valence electron would be in a π state and would not contribute at all to an effective electric field ($\cos\chi=0$). However, spin-orbit mixing with nearby $^2\Sigma$ states can introduce a σ electron, but its effective electric field is reduced by a factor of $\sin\chi$. This mixing is responsible for the large effective field in PbF because it has a very large spin-orbit constant. Finally, we arrive at the expression used to estimate the effective electric field in our approximation:

$$F_{\text{eff}} = \frac{\Delta E}{d_e} \approx -\left[\frac{4\sigma}{\sqrt{3}} h_0 \cos\chi \langle \text{mol},\sigma|\text{atom},s\rangle \times \langle \text{mol},\sigma|\text{atom},p\rangle \Gamma_{\text{rel}} \frac{Ze}{a_0^2}\right], \tag{22}$$

in terms of analytical expressions and concrete features of the MOLPRO output.

B. Potential curves

In the available literature, there is no consensus as to the true ground state of PtH^+ [17,30,31]; only one paper attempts to work out the ground state of HfH^+ [17]. The debate arises in PtH^+ concerning the ordering of the $^1\Sigma$ and $^3\Delta$ states. Therefore, we use MOLPRO along with state-of-the-art basis sets [32] to compute several electronic states of these molecules in addition to the $^3\Delta$ states of interest.

Diatomic molecules belong to the $C_{2\infty}$ point group; however, MOLPRO only uses Abelian point groups, necessitating the use of the C_{2v} point group for our calculations. In this point group, the projection of electronic angular momentum along the diatomic axis (Λ) will transform as the following: $\Lambda=2n$ will transform as $A1$ symmetry, $\Lambda=-2n$ as $A2$, $\Lambda=2n+1$ as $B1$, and $\Lambda=-(2n+1)$ as $B2$. As a result, the full Δ symmetry transforms as $A1\oplus A2$, requiring the MOLPRO calculations to include both the $A1$ and $A2$ symmetries.

The MRCI [28,29] calculations are performed after a MCSCF [26,27] calculation at various internuclear separations ($1\ \text{Å} < r < 7\ \text{Å}$). The term "active space" describes the set of orbitals being used to construct the configurations, as in Eq. (18). The active space is increased in one of two ways. One is to allow the electrons to reside in higher-lying orbitals that are nominally unoccupied. The second is to promote electrons from previously closed shells into these same orbitals. Both of these options allow more parameters with which to optimize the total energy, but it comes at the expense of an increased computational burden.

The basis sets and active space sizes are bench-marked against the dissociation energies of [17,30,31]. Our final choice was the ECP60MWB basis built and defined by the Stuttgart/Cologne group [33] for the heavy atom along with the standard aug-cc-pVTZ basis [34] for the hydrogen. The MWB bases of the Stuttgart/Cologne [32,33] group stand for neutral atom quasirelativistic potentials. To make calculations manageable, these basis sets deal explicitly only with electrons outside of a 60-electron "core." The effect of these core electrons is incorporated through an effective core potential (ECP), which is also provided along with the basis sets. The ECP's include angular-averaged (i.e., scalar) relativistic effects.

The active space chosen is of the form $(A1,B1,B2,A2)=(6,2,2,1)$ for both PtH^+ and HfH^+. This notation means that the first 6 $A1$, 2 $B1$, 2 $B2$, and 1 $A2$ orbitals above the closed space are active. In PtH^+ and HfH^+, we close off orbitals in (2,1,1,0). Closed orbitals participate in optimizing the energy subject to the constraint that they are always doubly occupied. Thus, they do not participate in correlations. These calculations resulted in dissociation energies of 3.14 eV (PtH^+) and 2.49 eV (HfH^+) compared to previous theoretical energies of 2.87 and 2.50 eV [17]. Dyall [30] obtains a dissociation energy for PtH^+ of 2.00 eV while Zurita *et al.* [31] obtain 2.22 eV, both of which are significantly smaller than our result. Our deeper, and presumably more accurate, dissociation energies are most likely due to increased computational efficiency over the past decade. Calculations on PtH^+ were completed in approximately 6 cpu h per point on a 2.4 GHz processor, while for HfH^+ they were completed in approximately 20 cpu min per point.

In order to further test the basis sets, we performed calculations on Pt and Hf to find the ionization energies. We ran a MCSCF/MRCI calculation on Pt, Pt^+, and Pt^{2+} as well as for Hf, Hf^+, and Hf^{2+}. We found the first and second ionization energies of Pt to be 65 000 and 14 3000 cm^{-1} and of Hf to be 49 600 and 115 500 cm^{-1}. They agree with the empirical values [19,35] to within 6000 cm^{-1}.

Born-Oppenheimer potential curves for several symmetries are presented in Fig. 1. The curves are generated by fitting an extended Rydberg function to the points obtained from the MOLPRO calculation, using the method of Ref. [36]. All curves shown dissociate to the ground ^2S state of H and the ^2D state of the transition metal ion. To assign a Hund's case (a) label to a curve, we consult the MOLPRO output and assign a value based on the CI eigenvector. In turn, the eigenvector tells in which orbitals the electrons lie. There are several different configurations present, but the dominant configuration has a coefficient h_0 very close to unity. As in the case of a PtH^+, we find there are several configurations, each having two unpaired electrons in the $A1$ symmetry group. Upon examining the orbitals where these electrons lie, we find one has an angular momentum projection $\lambda=0$, while the other has $\lambda=+2$. Hence, this is a $(\sigma\delta)$ configuration. Some CI vectors have the same unpaired electrons but have paired electrons in a different orbital and/or symmetry group. In our approximation, these paired electrons play no role, and therefore they contribute nothing to the effective electric field within the molecule. Last, if this configuration is truly a $^3\Delta$, there should be an equivalent energy configuration with one orbital in symmetry $A1$ and another in symmetry $A2$. This is indeed what we find.

Recall that Hund's case (a) describes a diatomic molecule with spin and orbital motion strongly coupled to the molecular axis. Hence the electronic part of the Hamiltonian is dominant followed by spin-orbit and then rotational coupling. Within the Hund's case (a) MRCI calculation, both molecules nominally possess $^1\Sigma$ ground states. However,

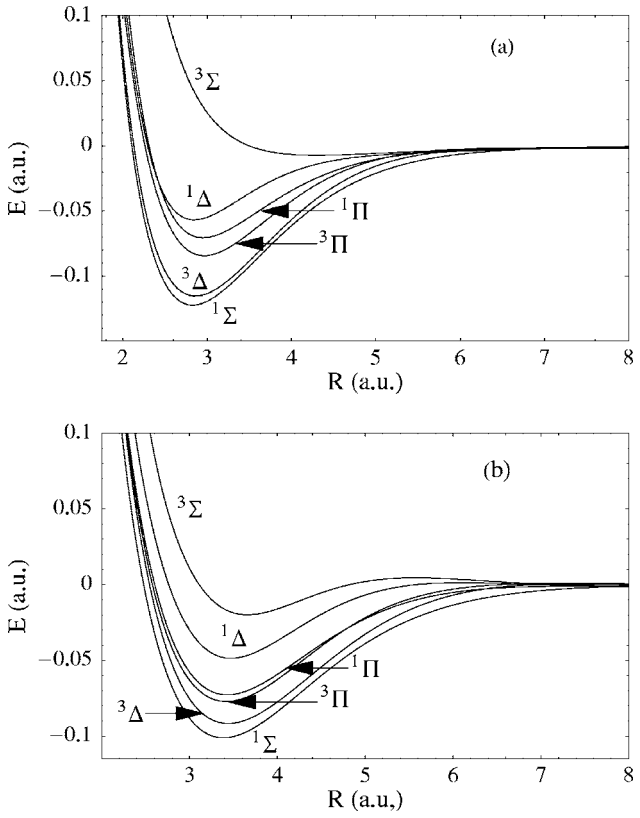

FIG. 1. Potential energy curves for PtH^+ (a) and HfH^+ (b), as obtained from the MOLPRO output.

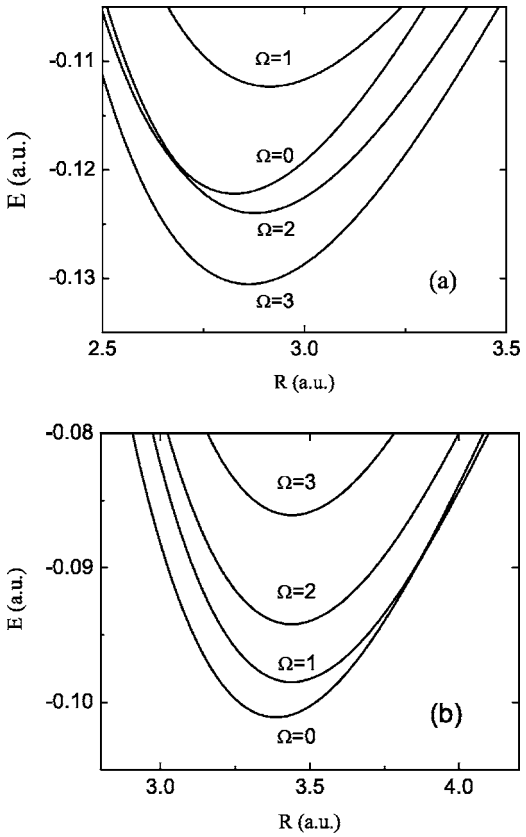

FIG. 2. Hund's case (c) potential curves for PtH^+ (a) and HfH^+ (b), labeled by the quantum number Ω. These curves are obtained from those in Fig. 1 by adding spin-orbit corrections perturbatively, as described in the text.

both have low-lying $^3\Delta$ states. The energy difference $E_{^3\Delta} - E_{^1\Sigma}$ is 1500 cm^{-1} for PtH^+ and 2100 cm^{-1} for HfH^+. At this level we therefore agree qualitatively with the ordering of states given by Ref. [17] for PtH^+, but not HfH^+. The equilibrium separations compare favorably to previous results for PtH^+ [17,30,31] and HfH^+ [17]. Rotational constants were not quoted in these papers. In the $^3\Delta$ states of PtH^+ and HfH^+ we find $r=1.51$ Å, $B_e=7.37 cm^{-1}$ and $r=1.82$ Å, and $B=5.11 cm^{-1}$.

C. Estimating diagonal spin-orbit contributions

Roughly speaking, the molecules inherit a large spin-orbit interaction from the heavy ion. Moreover, the spin-orbit constant A in PtH^+ is expected to be negative, as it is in the Pt^+ ion, thus shifting the $^3\Delta_3$ state lower in energy. For this reason it was previously anticipated that $^3\Delta_3$ is likely to be the absolute ground state of PtH^+ [30]. By contrast, in HfH^+, A is expected to be positive and hence the $^3\Delta_1$ state is shifted down in energy. To estimate the size of the shift, we require knowledge of A in both molecules. Using methods outlined in Ref. [23], we estimate the value of A using van Vleck's "pure precession hypothesis" [37]. Under this approximation, the spin-orbit coupling arises from the heavy atom, and the atomic orbital angular momentum l of each electron is taken to be a good quantum number.

Using this assumption, the "stretched state" $^3\Delta_3$ is represented by the following Slater determinant:

$$|^3\Delta_3\rangle = |d\delta^\alpha s\sigma^\alpha|. \tag{23}$$

In this expression, we make explicit the orbital angular momentum quantum numbers d and s; the index α stands for an electron spin aligned along the molecular axis, $\sigma=+\frac{1}{2}$. The other states can be generated from this one by the application of suitable spin-lowering operators. We can now act upon wave functions of this type with the single-electron–spin-orbit operator, by recasting it in terms of operators acting on the individual electrons i:

$$H^{LS} = A\mathbf{L}\cdot\mathbf{S} = \sum_i a_i \mathbf{l}_i \cdot \mathbf{s}_i. \tag{24}$$

Details of this procedure are presented in the Appendix. A more thorough treatment of spin-orbit and rotational coupling will be performed elsewhere [38].

The effect of the spin-orbit mixing is to break the degeneracy of the different Ω values and produce a revised set of potential curves, indexed by Hund's case (c) quantum numbers. These curves are shown in Fig. 2. Performing these calculations yields values of $A=-1680$ and $A=610$ cm^{-1} for the molecular spin-orbit constants of PtH^+ and HfH^+, respectively. This shift is more than enough to push the $^3\Delta_3$ curve below that of the $^1\Sigma$ in PtH^+ [Fig. 2(a)]. Recall that the $^1\Sigma$ state shifts little in energy because there is no spin or orbital motion, and therefore any shift in energy must be a second-

order effect. The lowest $\Omega=3$ curve is solely $^3\Delta_3$. Additionally, the $^3\Delta_3$ state of PtH^+ is well described in Hund's case (a); there are no other states with $\Omega=3$ nearby in energy (the closest we estimate is a $^3\Phi_3$ state $\approx 30\,000$ cm^{-1} away that dissociates to the ^{4}F limit of Pt^+).

The same results applied to HfH^+ tell a different story [Fig. 2(b)]. The value A is not sufficiently large to shift the $^3\Delta_1$ state below the $^1\Sigma_0$ state. The energy difference between $\Omega=1$ and $\Omega=0$ states is 600 cm^{-1}. There are other relativistic effects, such as the second-order correction to the spin-orbit constant and spin-spin and spin-rotation interactions, that can further push down the $^3\Delta_1$ state. For example, we can estimate the second-order–spin-spin parameter in terms of the atomic spin-orbit constant in the pure-precession approximation [23]. In these heavy elements it is the more dominant contribution to spin-spin. We find

$$\lambda^{(2)} = -\frac{|\langle {}^3\Delta_2|H_{so}|{}^1\Delta_2\rangle|^2}{E_{^3\Delta}-E_{^1\Delta}} = -\frac{1}{2}\frac{a^2}{E_{^3\Delta}-E_{^1\Delta}} \approx 60\ \text{cm}^{-1}. \tag{25}$$

These contribute to an uncertainty of an order of magnitude smaller than the energy difference in the spin-orbit-corrected curves. It is conceivable that the sum total of these other relativistic effects, acting more strongly on the $^3\Delta$ state than on the $^1\Sigma$ state, will reverse the ordering in Fig. 2(b). In principle, there is an uncertainty in the computed electronic energy using MOLPRO, but this is not trivial to estimate. States more subject to relativistic effects (such as $^3\Delta$) are less accurately computed compared to a $^1\Sigma$ state. More detailed calculations—or, even better, experiments—will be required to decide this issue.

If it turns out that the ground state of HfH^+ is $^1\Sigma$, then the $^3\Delta_1$ state is metastable, and an estimate of its lifetime is desirable. On symmetry grounds we see that this lifetime should be very long, because of the fact that the transition would require $\Delta S=1$, $\Delta\Omega=1$, and $\Delta\Lambda=2$. $\mathbf{J}$ is the total angular momentum about the internuclear axis, $\mathbf{J}=\mathbf{L}+\mathbf{S}+\mathbf{N}$, where $\mathbf{N}$ is the mechanical rotation of the nuclei about their center of mass. The S and Ω changes are not dipole allowed in the case (a) basis. However, rotational couplings do not preserve the value of Ω, and spin-orbit couplings do not preserve the value of S. Because of such interactions, the molecule is not a pure Hund's case (a) molecule. The $^3\Delta$ states may, therefore, be contaminated by small amplitudes of other case (a) states that are dipole allowed. These are very small effects and it is the reason that these terms are usually neglected in the Born-Oppenheimer approximation. For example, we can compute the amount of contamination of the $^1\Pi_1$ state in the $^3\Delta_1$ state via the spin orbit interaction. This was done to produce the curves in Fig. 2. Using the eigenvectors of the case (c) $\Omega=1$ functions we compute the lifetime to be ($|\Omega=1\rangle=\eta|^3\Delta_1\rangle+\zeta|^3\Pi_1\rangle+\xi|^1\Pi_1\rangle$):

$$\Gamma \approx \tfrac{4}{3}\xi^2\alpha^3(E_{^3\Delta_1}-E_{^1\Sigma_0})^3 \rightarrow \tau \sim 10\ \text{s}.$$

We see that the lifetime is on the order of seconds.

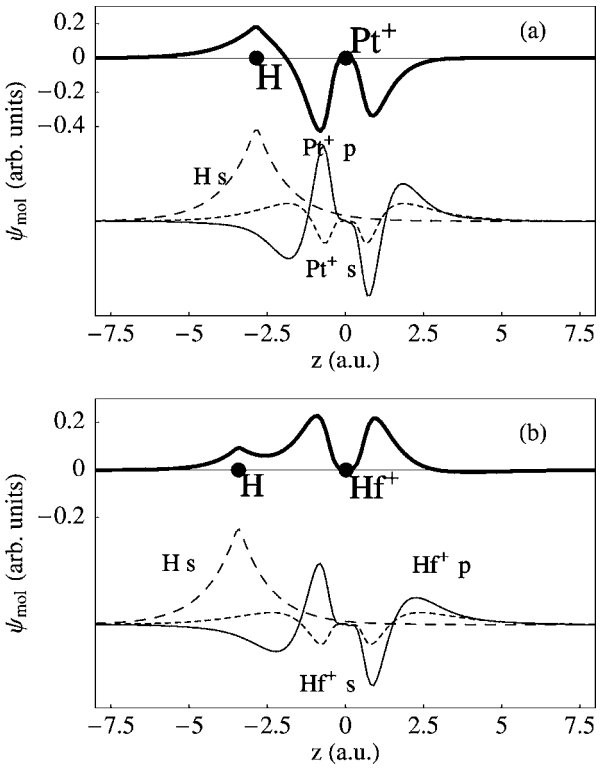

FIG. 3. Electronic wave functions (solid lines) for the relevant σ molecular orbitals in the PtH^+ (a) and HfH^+ (b) ions. In each figure, the lower panel shows the dominant s and p orbitals on the heavy ion, plus the s orbital on the hydrogen atom. All wave functions are normalized to unity. By projecting the molecular orbital onto the atomic orbitals, we find $\epsilon_s=0.75$, $\epsilon_p=0.19$ for PtH^+, and $\epsilon_s=0.79$, $\epsilon_p=0.09$ for HfH^+.

D. Estimating ϵ_s and ϵ_p; the effective electric field

As we have seen, the electric field inside a polar diatomic molecule is independent of the applied electric field, provided that the molecule is polarized. There is a relativistic enhancement factor determined from properties of the heavy atom and a projection of the electron spin, σ, onto the molecular axis. Now we must determine, according to our working formula Eq. (22), how much the s and p atomic orbitals are mixed because of the presence of the other atom.

The values of ϵ_s and ϵ_p are obtained from the molecular structure calculations, as described above. Wave functions generated for the σ molecular orbital (not to be confused with the electron-spin projection σ) are presented in Fig. 3. In each panel, the electronic wave function on the molecular axis is plotted as a function of z, the electron's coordinate along this axis (heavy line). For comparison, the s, p, and hydrogen atomic orbitals are also shown below the molecular orbital wave function. All wave functions are normalized to unity. Note that the HfH^+ molecular ion in Fig. 3(b) is not as strongly mixed as in the case of PtH^+. This small mixing manifests itself as a smaller effective electric field for HfH^+ (not just due to the Z difference of 78 to 72). Qualitatively, this asymmetry illustrates the degree of s-p mixing that is vital to the observed electron EDM shift. By taking appropriate overlaps of atomic and molecular wave functions, we

TABLE I. Comparisons of published values of F_{eff} to our results using *nonrelativistic* software.

Molecule	Published F_{eff} (GV/cm)	This work F_{eff} (GV/cm)
BaF	7.4[a]	5.1
YbF	26[b]	43
HgF	99[c]	68
PbF	−29[c]	−36.6
PbO	6.1[d], 26[e]	6.4
HBr^+	−0.02[f]	0.16
HI^+	−0.1[f],0.34[g]	0.57
PtH^+	N/A	73
HfH^+	N/A	−17

[a]Reference [11].
[b]Reference [6,7].
[c]Reference [10].
[d]Reference [5].
[e]Reference [46].
[f]Reference [12], "ionic."
[g]Reference [13].

construct the effective electric field as defined in Sec. III A.

To check the validity of this procedure we have performed the calculations of the expected electric field in molecules for which $\mathbf{F}_{\text{eff}}$ has already been published; e.g., the $^2\Sigma$ fluorides as well as the group *VII* hydrides and PbO in its metastable $a^3\Sigma$ state. Values of R (the internuclear separation) and term symbols are taken from the previous work on these molecules. Please see Ref. [11] for BaF, Ref. [10] for PbF and HgF, Refs. [12,13] for HI^+, Ref. [12] for $HrBr^+$, Refs. [6,7] for YbF, and Ref. [5] for PbO. We once again used the basis sets of the Stuttgart/Cologne [33] group for the heavy elements. Please see Ref. [39] for Ba, Ref. [40] for Br, Ref. [41] for I, Ref. [42] for Yb, Ref. [43] for Pb, and Ref. [32] for Pt, Hf, and Hg. The lighter elements H and F use the aug-cc-pVTZ basis [34]. These results are presented in Table I. Although the literature values vary by nearly two orders of magnitude, our present method tracks most of them to within a factor of 2.

The lone exception is HBr^+. The sign discrepancy between our value and that in Ref. [12] is analogous to the sign difference in HI^+, as pointed out in Ref. [13]. Differences in the magnitude are likely due to use of an "ionic" bond Ref. [12], whereas HBr^+ is neither purely ionic nor covalent. Our method assumes nothing about the nature of the bond; rather, it allows the molecular structure software to calculate the electron distribution in the molecule and then projects the distribution onto atomic orbitals of the heavy atom.

The values we obtain for the effective electric fields are 73 GV/cm in the $^3\Delta_3$ state of PtH^+ and −17 GV/cm in the $^3\Delta_1$ state of HfH^+. Strikingly, these estimates are competitive with the largest ones previously identified. This result points to the imperative need for a complete electronic structure calculation to refine the predictions for these ions.

E. Ω doubling and critical fields

There remains the question of how easily polarized are the molecular states we have identified. The energy difference between states of differing parity Eq. (13) in a Δ state is a fourth-order effect in perturbation theory provided the $^{2S+1}\Pi$ and $^{2S+1}\Sigma$ electronic states are fairly well separated in energy from the $^{2S+1}\Delta$ state. Brown *et al.* [44] have used this idea to give formulas for estimating the effect in a manner consistent with the ideas of Mulliken and Christy [45], who worked out the effect in $^2\Pi$ states. Thus, the Ω doubling is relegated to finding the Λ doubling (the difference in energy between parity states comprised of $\Lambda=2$ and $\Lambda=-2$).

In a $^3\Delta$ state, there are three parameters contributing to the energy splitting designated $\tilde{o}_\Delta$, $\tilde{p}_\Delta$, and $\tilde{q}_\Delta$. The parameters have the following forms:

$$\tilde{o}_\Delta = 4\sqrt{30}\frac{V_A V_A V_B V_B}{\Delta E_1 \Delta E_2 \Delta E_3}\begin{Bmatrix} S & S & 2 \\ 1 & 1 & S' \end{Bmatrix}\frac{(2S-2)!}{(2S+3)!}, \quad (26)$$

$$\tilde{p}_\Delta = 4\sqrt{35}\frac{V_A V_B V_B V_B}{\Delta E_1 \Delta E_2 \Delta E_3}, \quad (27)$$

$$\tilde{q}_\Delta = 8\frac{V_B V_B V_B V_B}{\Delta E_1 \Delta E_2 \Delta E_3}, \quad (28)$$

where $V_{A(B)}$ is the matrix element of the spin-orbit (rotational) Hamiltonian between differing states. $\langle {}^3\Delta_1 | AL_- | {}^3\Pi_1 \rangle$ is an example of V_A, whereas $\langle {}^3\Delta_1 | BL_- | {}^3\Pi_0 \rangle$ is an example of V_B. The ΔE_i are the energy differences between the state of interest and the intermediate states. It is now straightforward to estimate the order of magnitude of E_{doub} in the $^3\Delta$ states.

In HfH^+, we are concerned with the $\Omega=1$ state, governed by the $\tilde{o}_\Delta$ parameter. We find E_{doub} to be (recall that $J=1$ in the ground state)

$$E_{doub}^{\Omega=1} = 2\tilde{o}_\Delta J(J+1) \approx \frac{8/6 \times 5!\sqrt{30}A^2B^2}{(E_{^3\Delta} - E_{^3\Pi})^2(E_{^3\Delta} - E_{^1\Sigma})}J(J+1)$$
$$= 5.1 \times 10^{-5}\ \text{cm}^{-1}.$$

This E_{doub} leads to an $\mathbf{F}_{\text{crit}} \approx 1$ V/cm using the value of $d_m = 2.92$ Debye obtained via the MOLPRO calculations. PtH^+ is slightly more complicated. The parameter governing its splitting is $\tilde{q}_\Delta$ and connects the $^3\Delta_1$ state to the $^3\Delta_3$ state. So, we first find the value of the parameter and then use second-order perturbation theory within the $^3\Delta_\Omega$ manifold. Thus we find (with $J=3$ in the ground state) that

$$E_{doub}^{\Omega=3} = \frac{2q^2 o[J(J+1)]^3[J(J+1)-2][J(J+1)-6]}{(4A-8B)^2}$$
$$\approx \frac{4 \times 10^5 B^{10} A^2}{(4A-8B)^2(E_{^3\Delta} - E_{^3\Pi})^6(E_{^3\Delta} - E_{^1\Sigma})^3}$$
$$= 3.32 \times 10^{-20}\ \text{cm}^{-1}.$$

Using $d_m = 0.77$ D in PtH^+, from the MOLPRO calculation, we find $\mathbf{F}_{crit} \approx 10^{-15}$ V/cm, which is negligible for any purpose.

IV. CONCLUSIONS

The $^3\Delta$ states of PtH^+ and HfH^+ satisfy our two most important criteria for experimental searches of the electron EDM. Both are easily polarized and expected to generate very high effective internal electric fields. However, several other experimentally relevant concerns remain to be resolved for these molecules, including: (1) whether $^3\Delta_1$ is the true ground state of HfH^+; (2) at what laser wavelengths the molecules can be probed and detected; and (3) how their magnetic properties, e.g., g factors, are influenced by channel couplings engendered by electric and magnetic fields and terms neglected in the Born-Oppenheimer approximation; i.e., intermediate coupling via J^+S^-, etc. These items demand further detailed study, and will be the subject of future work.

We have endeavored to articulate a strategy for estimating the influence of the electron EDM on molecular structure, using perturbation theory and nonrelativistic electronic structure calculation. This strategy has proved quite successful and should be useful to anyone wishing to assess the viability of a candidate molecule in the future. This estimate does not, of course, take the place of a complete relativistic many-electron calculation, which must be done as a follow-up.

Note added in proof. Finally, at the suggestion of E. Cornell's group, we have used the same methods to estimate the effective electric field for HfF^+. Like HfH^+, its ground state is a toss-up between $^3\Delta_1$ and $^1\Sigma$, and its effective electric field is $F_{\mathrm{eff}} \approx -18$ GV/cm.

ACKNOWLEDGMENTS

We gratefully acknowledge useful conversations with E. Cornell, A. Leanhardt, L. Sinclair, and R. Stutz and thank them for bringing the topic to our attention. We are also indebted to L. Gagliardi for discussions on PtH^+. E.R.M. thanks M. Thompson for some useful discussions pertaining to the MOLPRO software suite for heavy atoms. This work was supported by the NSF, the OSEP program at the University of Colorado, and the W. M. Keck Foundation.

APPENDIX: SPIN ORBIT IN VAN VLECK APPROXIMATION

First we calculate in terms of Hund's case (a) functions and then in terms of the single-electron operators. We present the wave functions in terms of Hund's case (a) numbers. These are presented by $|\Lambda;S,\Sigma;J,\Omega\rangle$ with $J \geqslant \Omega$. In terms of Slater determinants, the molecular wave functions are

$$|^3\Delta_3\rangle = |2;1,1;J,3\rangle = |d\delta^\alpha s\sigma^\alpha|, \tag{A1}$$

$$|^3\Delta_2\rangle = |2;1,0;J,2\rangle = \frac{1}{\sqrt{2}}(|d\delta^\alpha s\sigma^\beta| + |d\delta^\beta s\sigma^\alpha|), \tag{A2}$$

$$|^3\Delta_1\rangle = |2;1,-1;J,1\rangle = |d\delta^\beta s\sigma^\beta|, \tag{A3}$$

$$|^3\Pi_2\rangle = |1;1,1;J,2\rangle = |d\pi^\alpha s\sigma^\alpha|. \tag{A4}$$

Once again normalizations are assumed in the determinants. The spin-orbit energy shift for the $^3\Delta_3$ is then

$$\langle ^3\Delta_3|AL_zS_z|^3\Delta_3\rangle = 2A, \tag{A5}$$

$$\langle |d\delta^\alpha s\sigma^\alpha| a(l_1^z s_1^z + l_2^z s_2^z) \| d\delta^\alpha s\sigma^\alpha|\rangle = a\left[2\left(\tfrac{1}{2}\right) + 0\left(\tfrac{1}{2}\right)\right] = a. \tag{A6}$$

Now we apply the total spin lowering operator (given by $S_- = \Sigma_i s_i^-$) to Eq. (A1) to obtain the $^3\Delta_2$ state. Since the projection of the spin, Σ, is zero, there is no shift. Therefore, the molecular spin-orbital constant A is half the atomic spin-orbit constant a. The spin-orbit parameter is the same for all states within the $^3\Delta$ manifold.

There are higher-order effects via coupling to other $\Omega = 3$ electronic states. Yet, the only other $\Omega = 3$ states come from $^3\Phi$ or $^5\Phi$ states, which lie far off in energy. They can be evaluated to see the second-order contribution to the molecular spin-orbit constant via a calculation similar to the one below describing the coupling of $\Omega = 2$ states.

Off-diagonal effects of spin orbits can be evaluated using the same one-electron operators. First we write the off diagonal elements using spherical tensor notation.

$$\frac{a}{2}\sum_{q=\pm 1} l_1^q s_1^{-q} + l_2^q s_2^{-q}. \tag{A7}$$

Then we evaluate the coupling between Eqs. (A2) and (A4). The only one-electron element that works is $l_1^+ s_1^-$ to take $^3\Pi_2$ to $^3\Delta_2$. Only including the terms that contribute, we find

$$\left\langle \frac{|d\delta^\beta s\sigma^\alpha|}{\sqrt{2}} \middle| \frac{a}{2} l_1^+ s_1^- \middle| |d\pi^\alpha s\sigma^\alpha|\right\rangle = \frac{a}{2\sqrt{2}}\sqrt{(6-2)(3/4+1/4)} = \frac{a}{\sqrt{2}}. \tag{A8}$$

These calculations take into account the permutations of the indices within the determinant. This is what cancels the normalization. We have ignored the effects of the other electrons in the Slater determinant that belong to paired orbitals. These can, in principle, contribute via permutations of the indices and raising and/or lowering the angular momentum. These types of contributions will be evaluated in future studies.

[1] S. M. Barr, Int. J. Mod. Phys. A **8**, 209 (1993).
[2] B. C. Regan, E. D. Commins, C. J. Schmidt, and D. DeMille, Phys. Rev. Lett. **88**, 071805 (2002).
[3] P. G. H. Sandars, Phys. Lett. **14**, 194 (1965).
[4] M. G. Kozlov and D. DeMille, Phys. Rev. Lett. **89**, 133001 (2002).
[5] D. DeMille, F. Bay, S. Bickman, D. Kawall, D. Krause, S. E. Maxwell, and L. R. Hunter, Phys. Rev. A **61**, 052507 (2000).

[6] J. J. Hudson, B. E. Sauer, M. R. Tarbutt, and E. A. Hinds, Phys. Rev. Lett. **89**, 023003 (2002).
[7] M. G. Kozlov and V. F. Ezhov, Phys. Rev. A **49**, 4502 (1994); M. G. Kozlov, J. Phys. B **30**, L607 (1997); F. A. Parpia, *ibid.* **31**, 1409 (1998).
[8] V. A. Dzuba, V. V. Flambaum, J. S. M. Ginges, and M. G. Kozlov, Phys. Rev. A **66**, 012111 (2002).
[9] H. M. Quiney, J. K. Laerdahl, K. Fægri, Jr., and T. Saue, Phys. Rev. A **57**, 920 (1998).
[10] Yu. Yu. Dmitriev, Yu. G. Khait, M. G. Kozlov, L. N. Labzovsky, A. O. Mitrushenkov, A. V. Shtoff, and A. V. Titov, Phys. Lett. A **167**, 280 (1992).
[11] M. G. Kozlov, A. V. Titov, N. S. Mosyagin, and P. V. Souchko, Phys. Rev. A **56**, R3326 (1997).
[12] B. Ravaine, S. G. Porsev, and A. Derevianko, Phys. Rev. Lett. **94**, 013001 (2005).
[13] T. A. Isaev, N. S. Mosyagin, A. N. Petrov, and A. V. Titov, Phys. Rev. Lett. **95**, 163004 (2005).
[14] R. Sinclair, J. Bohn, A. Leanhardt, P. Maletinsky, E. Meyer, R. Stutz, and E. Cornell, Bull. Am. Phys. Soc. **50**, 134 (2005).
[15] L. Sinclair *et al.*, DAMOP05 Abstract M6.00119 (2005).
[16] L. I. Schiff, Phys. Rev. **132**, 2194 (1963).
[17] G. Ohanessian, M. J. Brusich, and W. A. Goddard III, J. Am. Chem. Soc. **112**, 7179 (1990).
[18] I. B. Khriplovich, *Parity Nonconservation in Atomic Phenomena* (OPA, Amsterdam, 1991).
[19] C. E. Moore, *Atomic Energy Levels*, NBS Monogr. Circ. No. 467 (U. S. GPO, Washington, D. C., 1958), Vols. I–III.
[20] M. G. Kozlov and L. N. Labzowski, J. Phys. B **28**, 1933 (1995).
[21] V. V. Flambaum and D. W. Murray, Phys. Rev. A **55**, 1736 (1997).
[22] I. B. Khriplovich and S. K. Lamoreaux, *CP Violation without Strangeness* (Springer-Verlag, Berlin, 1997).
[23] J. Brown and A. Carrington, *Rotational Spectroscopy of Diatomic Molecules* (Press Syndicate of the University of Cambridge, Cambridge, 2003).
[24] M. J. Frisch *et al.*, GAUSSIAN 98 (Revision A. x) (Gaussian, Inc., Pittsburgh, PA, 1998).
[25] MOLPRO, version 2002.6, a package of *ab initio* programs; H.-J. Werner, P. J. Knowles, and R. Lindh *et al.* (see http://www.molpro.net), Birmingham, UK, 2003.
[26] H. Werner and P. J. Knowles, J. Chem. Phys. **82**, 5053 (1985).
[27] P. J. Knowles and H. Werner, Chem. Phys. Lett. **115**, 259 (1985).
[28] H. Werner and P. J. Knowles, J. Chem. Phys. **89**, 5803 (1988).
[29] P. J. Knowles and H. Werner, Chem. Phys. Lett. **145**, 514 (1988).
[30] K. G. Dyall, J. Chem. Phys. **98**, 9678 (1993).
[31] S. Zurita, J. Rubio, F. Illas, and J. C. Barthelat, J. Chem. Phys. **104**, 8500 (1996).
[32] D. Andrae, U. Haeussermann, M. Dolg, H. Stoll, and H. Preuss, Theor. Chim. Acta **77**, 123 (1990).
[33] H. Stoll, B. Metz, and M. Dolg, J. Comput. Chem. **23**, 767 (2002).
[34] T. H. Dunning, Jr., J. Chem. Phys. **90**, 1007 (1989); J. M. L. Martin and A. Sundermann, *ibid.* **114**, 3408 (2001).
[35] J. Blaise and J.-F. Wyart, J. Res. Natl. Inst. Stand. Technol. **97**, 217 (1992).
[36] A. Aguado and M. Paniagua, J. Chem. Phys. **96**, 1265 (1992).
[37] J. H. Van Vleck, Phys. Rev. **33**, 467 (1929).
[38] E. R. Meyer (unpublished).
[39] M. Kaupp, P. V. R. Schleyer, H. Stoll, and H. Preuss, J. Chem. Phys. **94**, 1360 (1991).
[40] A. Bergner, M. Dolg, W. Kuechle, H. Stoll, and H. Preuss, Mol. Phys. **80**, 1431 (1993).
[41] H. Stoll, B. Metz, and M. Dolg, J. Comput. Chem. **23**, 767 (2002).
[42] M. Dolg, H. Stoll, A. Savin, and H. Preuss, Theor. Chim. Acta **75**, 173 (1989). M. Dolg, H. Stoll, and H. Preuss, *ibid.* **85**, 441 (1993).
[43] B. Metz, H. Stoll, and M. Dolg, J. Chem. Phys. **113**, 2563 (2000); K. A. Peterson, *ibid.* **119**, 11099 (2003).
[44] J. M. Brown, A. S.-C. Cheung, and A. J. Merer, J. Mol. Spectrosc. **124**, 464 (1987).
[45] R. S. Mulliken and A. Christy, Phys. Rev. **38**, 87 (1931).
[46] A. N. Petrov, A. V. Titov, T. A. Isaev, N. S. Mosyagin, and D. DeMille, Phys. Rev. A **72**, 022505 (2005).